Optimal number and placement of piezoelectric sensor/actuator pairs for active vibration control

Project report by:

Vinod Kumar Singla (#200149761)

May 1, 2017

TABLE OF CONTENTS

LIST OF TABLES

LIST OF FIGURES

ABSTRACT

Optimal vibration suppression of a beam using collocated piezoelectric sensor/actuator pairs was investigated in this project. A state space model for simulating time response of first four modes of a beam with up to three piezoelectric sensor/actuator pairs was developed. Total integrated energy stored in the system was minimized by varying the position of piezoelectric patches of constant length while keeping feedback gains constant using genetic algorithm. Peak modal time response amplitude after 1 second was compared for first four vibration modes with different number of patches. Finally, the improvement in vibration suppression obtained by increasing number of piezoelectric patches was tabulated to get a sense of the tradeoff associated with cost and performance.

1 INTRODUCTION

Vibration reduction of flexible structures using piezoelectric sensors and actuators has received considerable interest in recent years. This can be attributed to the fact that piezoelectric materials have excellent electromechanical properties: fast response, easy fabrication, design flexibility, low weight, low cost, large operating bandwidth, low power consumption and generation of no magnetic field while converting electrical energy into mechanical energy [1]. Vibration reduction using piezoelectric materials is often termed as 'active vibration control'.

Crawley et al. [2] studied the performance of active vibration control depending not just on the control law but also on judicious placement of piezoelectric sensors and actuators. Since then, a number of approaches for optimal placement of piezoelectric sensors and actuators have been presented in the literature depending upon the end application. Gupta et al. [1] presented the most commonly used criteria among researchers. These included maximizing modal forces/moments applied by piezoelectric actuators, maximizing deflection of the host structure, minimizing control effort/maximizing energy dissipated, maximizing degree of controllability, maximizing degree of observability, and minimizing spill-over effects.

Much of the work for optimal placement of piezoelectric sensors and actuators on a cantilever beam arbitrarily assumes a fixed number of standard sensor/actuator pairs during problem formulation. This leads to a question whether the same vibration reduction performance for a particular configuration can be achieved with lesser number of appropriately positioned sensors/actuators and adjusting the settings of the controller. The problem of optimal number and placement of sensor/actuator pairs has been considered for plates [3], multistory buildings [4] and trusses [5] in the past. A similar treatment for optimal number & placement of piezoelectric sensors/actuators on a simply supported beam is considered in this project. The objectives of this project are: 1) To obtain optimal geometric distribution of piezoelectric patches by maximizing energy dissipation through genetic algorithm 2) To quantify improvement in vibration suppression obtained by increasing number of piezoelectric patches to get a sense of the tradeoffs associated with cost and performance.

2 BEAM MODEL WITH SENSORS/ACTUATORS

A beam model bonded with piezoelectric actuators on the upper surface and sensors on the lower surface considered for this analysis is shown in Figure 1. The sensors and actuators are geometrically positioned to be collocated with each other as this guarantees stability of the closed loop system. There are *m* sensor/actuator pairs (for a total of 2*m* piezoelectric patches) bonded on the surface of the beam. The patches are assumed to be polarized in the *z* direction.
The equation of motion for the beam with when external charges are applied on the piezoelectric actuators is given by [6]:

$$Y_b I_b \frac{\partial^4 w}{\partial x^4} + \rho_b A_b \frac{\partial^2 w}{\partial t^2} - b \sum_{i=1}^{m} \frac{\partial^2 M_i^a}{\partial x^2} = 0 \tag{1}$$

where

w is the deflection of the beam

Y_b is the young's modulus of the beam

I_b is the moment of inertia of the beam

ρ_b is the material density of the beam

b is the width of the beam

A_b is the area of cross-section of the beam

Also, M_i^a is the moment on the beam by the force exerted by actuator i and is given as:

$$M_i^a = r^a d_{31} Y_p \phi_i^a(x,t) \tag{2}$$

where

d_{31} is piezoelectric strain constant of the actuators

Y_p is young's modulus of the actuators

ϕ_i^a is the voltage applied to the actuator i

r^a is the distance between midplane of the actuator to neutral surface of the beam

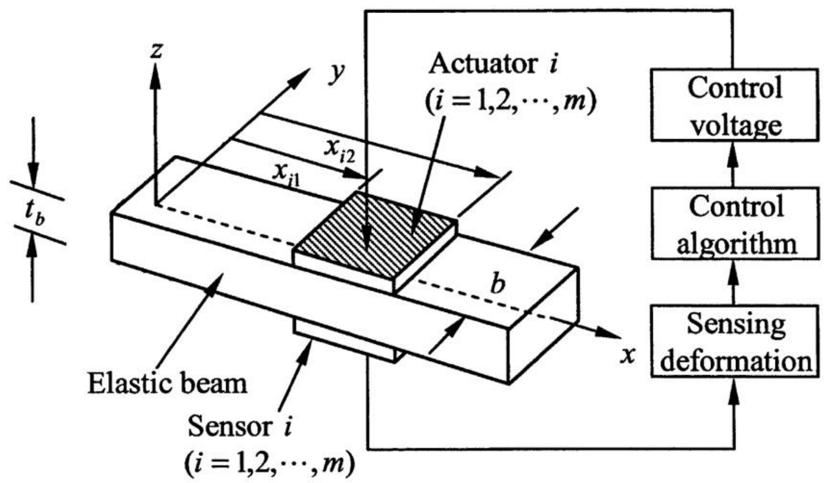

Figure 1. Beam model with sensors/actuators [8]

The distribution of voltage across actuator i is given by:

$$\phi_i^a(x,t) = \phi_i^a(t)[H(x - x_{i1}) - H(x - x_{i2})] \tag{3}$$

where

H(.) is the Heaviside step function

x_{i1}, x_{i2} start and finish coordinates of actuator i

Utilizing modal decomposition method for n modes, we can write the deflection w of the beam as:

$$w(x,t) = \sum_{j=1}^{n} U_j(x)\eta_j(t) \tag{4}$$

where

$U_j(x)$ is the j[th] normalized orthogonal mode shape

$\eta_j(t)$ is the j[th] modal amplitude

Substituting eqns. (2) - (4) into eqn. (1) and solving for the j[th] mode, we get:

$$\ddot{\eta}_j(t) + \omega_j^2\eta_j(t) = K_a\left[U_j'(x_{i2}) - U_j'(x_{i1})\right]\phi_i^a(t) \quad (j = 1, 2, \ldots, n) \tag{5}$$

Also, natural frequency of j^th mode can be calculated as:

$$\omega_j^2 = \int_0^L Y_b I_b U_j'' U_j'' dx \tag{6}$$

where

ω_j is the natural frequency of j^th mode
L is the length of the beam
$K_a = br^a d_{31} Y_p$
$(')$ is derivative of the function
$('')$ is double derivative of the function

The expression for average i^th sensor output voltage is given by:

$$\phi_i^s(x,t) = -\frac{bt^s}{S^e}\int_{x_{i1}}^{x_{i2}}\left(h_{31} r^s \frac{\partial^2 w}{\partial x^2}\right) dx = K_s \sum_{j=1}^{n}\left[U_j'(x_{i2}) - U_j'(x_{i1})\right]\eta_j(t) \tag{7}$$

where

$K_s = -\frac{t^s}{x_{i2}-x_{i1}} h_{31} r^s$
t^s is the thickness of the sensor
h_{31} is the piezoelectric constant
r^s distance between midplane of the sensor to neutral surface of the beam

Assuming a state vector of the form $\underline{x} = [\,\eta_1, \eta_2, \eta_3, \eta_4, \dot{\eta_1}, \dot{\eta_2}, \dot{\eta_3}, \dot{\eta_n}]^T$, we can transform the vibration and sensing equations (5) and (7) into a state space model given by:

$$\underline{\dot{x}} = A\underline{x} + B\underline{\phi_a} \tag{8}$$

$$\underline{\phi_s} = C\underline{x} \tag{9}$$

where

$$A = \begin{bmatrix} 0_{nxn} & I_{nxn} \\ -\omega^2 & -2\zeta\omega \end{bmatrix} \tag{10}$$

$$B = \begin{bmatrix} 0_{nxm} \\ B^* \end{bmatrix} \tag{11}$$

$$C = [C^* \quad 0_{mxn}], \tag{12}$$

$$B^* = \begin{bmatrix} B_{11} & B_{12} \dots & B_{1m} \\ B_{21} & B_{22} \dots & B_{2m} \\ & . & \\ & . & \\ & . & \\ B_{n1} & B_{n2} \dots & B_{nm} \end{bmatrix}, \tag{13}$$

$$C^* = \begin{bmatrix} C_{11} & C_{12} \dots & C_{1n} \\ C_{21} & C_{22} \dots & C_{2n} \\ & . & \\ & . & \\ & . & \\ C_{m1} & C_{m2} \dots & C_{mn} \end{bmatrix}, \tag{14}$$

$$B_{ji} = K_a[U_j'(x_{i2}) - U_j'(x_{i1})], \tag{15}$$

$$C_{ij} = K_s[U_j'(x_{i2}) - U_j'(x_{i1})], \tag{16}$$

$$\underline{\phi}_a = \begin{bmatrix} \phi_a^1 \\ \phi_a^2 \\ \vdots \\ . \\ \phi_a^m \end{bmatrix}, \tag{17}$$

$$\underline{\phi}_s = \begin{bmatrix} \phi_s^1 \\ \phi_s^2 \\ \vdots \\ . \\ \phi_s^m \end{bmatrix} \tag{18}$$

$$\omega = \begin{bmatrix} \omega_1 & & \\ & \ddots & \\ & & \omega_n \end{bmatrix}, \tag{19}$$

$$\zeta = \begin{bmatrix} \zeta_1 & & \\ & \ddots & \\ & & \zeta_n \end{bmatrix} \tag{20}$$

ζ_j is j[th] mode damping ratio

3 DESIGN OPTIMIZATION

For the vibration suppression of flexible systems, the total energy stored in the system can be considered as a representation of the vibration response [9]. Minimizing the total integrated energy stored in the system has the same effect as maximization of energy dissipated.

For the state space model considered in Section 2, if negative velocity feedback is considered for actuator voltage we can write:

$$\phi_a = -G_s\dot{\phi}_s = GC\underline{\dot{x}} \tag{21}$$

where G is the feedback gain matrix. The closed-loop state space equation then becomes:

$$\underline{\dot{x}} = A_{cl}\underline{x} \tag{22}$$

where

$$A_{cl} = \begin{bmatrix} 0_{nxn} & I_{nxn} \\ -\omega^2 & -B^*GC^* - 2\zeta\omega \end{bmatrix} \tag{23}$$

The integrated total energy stored in the system is then given by:

$$E = \int_0^\infty x^T Q x dt \tag{24}$$

where

$$Q = \begin{bmatrix} \omega^2 & 0 \\ 0 & I_{nxn} \end{bmatrix} \tag{25}$$

The application of standard state transformation techniques to eqn. (24) gives:

$$E = -x^T(t_0)Px(t_0) \tag{26}$$

where $x^T(t_0)$ is the initial state and P is the solution of the below Lyapunov equation:

$$A_{cl}^T P + PA_{cl} = Q \tag{27}$$

Observe that the total integrated energy is an implicit function of feedback gain matrix, G and position of sensor/actuator pairs. Therefore, by minimizing the total integrated energy stored in the system for a particular set of gains, we can obtain the optimal geometric distribution of the sensors/actuators.

The optimization problem in standard form can then be written as:

$$\text{Minimize } E(\underline{x}, G)$$

Subject to:

$$0 \le x_{i1}, x_{i2} \le L \qquad (i = 1,2, \ldots, m)$$

$$x_{i1} - x_{i2} \le 0 \qquad (i, j = 1,2, \ldots, m)$$

$$G_{ij} \le G_u \qquad (i, j = 1,2, \ldots, m)$$

$$x_{i2} - x_{(i+1)1} \le 0 \qquad (i = 1,2, \ldots, m-1)$$

$$G_{ij} \in G$$

where G_u is the upper limit for the individual gain elements in G matrix. Since the problem is highly non-linear, a genetic algorithm (GA) is used for solution of the optimization problem. The pseudo code [11] is given below:

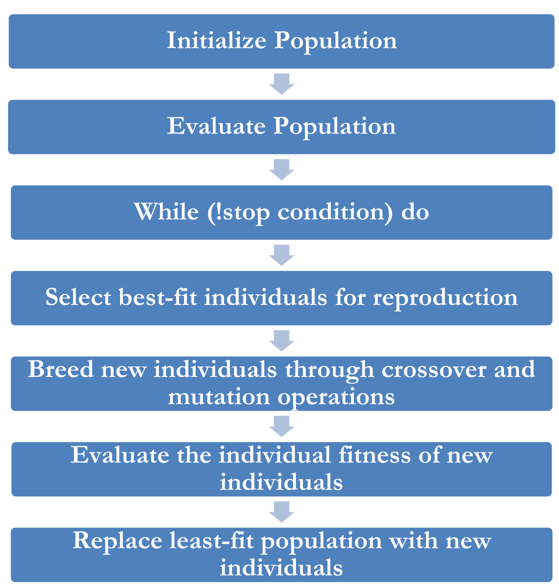

Figure 2. Pseudo code for genetic algorithm

4 IMPLEMENTATION & RESULTS

Based on the model formulation and optimization criterion presented in Section 2 and Section 3 respectively, optimal vibration control for initial condition response of a simply supported beam was performed. The specifications of piezoelectric patches and beam utilized for analysis are given in Table 1 below. In this analysis, first four vibration modes are considered with up to 3 sensor/actuator pairs. The initial conditions of the state vector are chosen in such a way that first four vibration modes have roughly the same amount of kinetic energy stored in the system if no control is applied and are given below:

$$\underline{x}(t_0) = [0\ 0\ 0\ 0\ 0.2\ 0.4\ 0.6\ 0.8]$$

Table 1. Structure and piezoelectric patch specifications

Item	**Beam**	**Actuators**	**Sensors**
Mass density (kg/m^3)	1190	1800	1800
Young's modulus (GPa)	3.1028	2	2
Poisson's ratio	0.3	0.3	0.3
Piezoelectric constant d_{31} (m/V)		2.3 X 10^{-11}	2.3 X 10^{-11}
Piezoelectric constant h_{31} (V/m)			4.32 X 10^{8}
Thickness (m)	1.6 X 10^{-3}	4 X 10^{-5}	4 X 10^{-5}
Length (m)	0.5		
Width (m)	0.01		
Damping ratio	0.01		

For a simply supported beam the mode shapes and natural frequencies are given by:

$$U_j(x) = \sqrt{\left[\frac{2}{\rho_b A_b L}\right]} \sin\left(\frac{j\pi x}{L}\right) \qquad (j = 1, 2, \dots, n) \tag{28}$$

$$\omega_j = \left(\frac{j\pi}{L}\right)^2 \sqrt{\frac{Y_b I_b}{\rho_b A_b}} \qquad (j = 1, 2, \dots, n) \tag{29}$$

Since, the optimization problem is highly non-linear as mentioned in earlier in Section 3, a robust heuristic search approach based on genetic algorithm is utilized for optimization. The GA settings utilized for optimization are given in Table 2 below:

Table 2. GA control settings

Item	**Value**
Population size	60
Crossover probability	0.8
Mutation probability	0.01
Maximum number of generations	200

The optimization algorithm was run several times for all three cases (one to three patch pairs) and results were tabulated for optimal patch locations (see Appendix B). The designs with least objective function value were selected and are shown in Table 3.

Table 3. Optimal patch locations

Number of patch pairs, m	**Placement of patches, x_{i1} - x_{i2} (m)**	**Feedback gain matrix, G**	**Objective function, E**
1	0.0268 – 0.1268	$[0.4]$	0.1922
2	0.0264 – 0.1264 0.302 – 0.402	$\begin{bmatrix} 0.4 & 0.4 \\ 0 & 0.4 \end{bmatrix}$	0.1659
3	0.0326 – 0.1326 0.1406 – 0.2406 0.3661 – 0.4661	$\begin{bmatrix} 0.4 & 0 & 0 \\ 0 & 0.4 & 0.0342 \\ 0 & 0 & 0.4 \end{bmatrix}$	0.1393

After determining the optimal patch locations for each of the cases considered, initial condition response of first four vibration modes with and without control using up to three sensor/actuator pairs was plotted and is shown in Figs. 3-6.

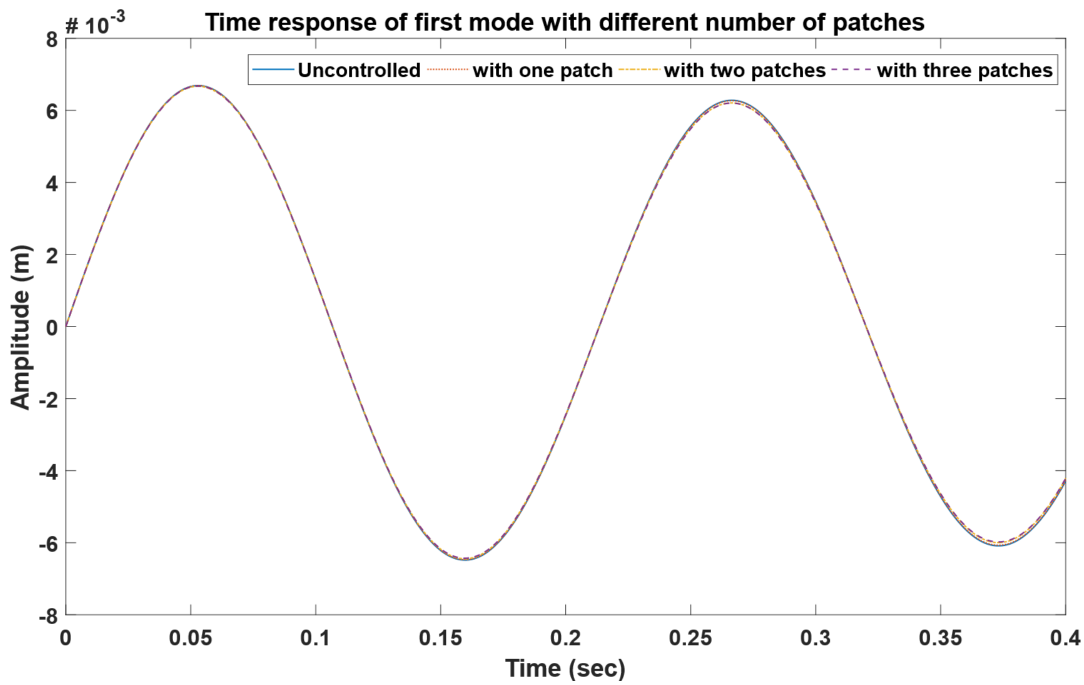

Figure 3. Time response of first mode

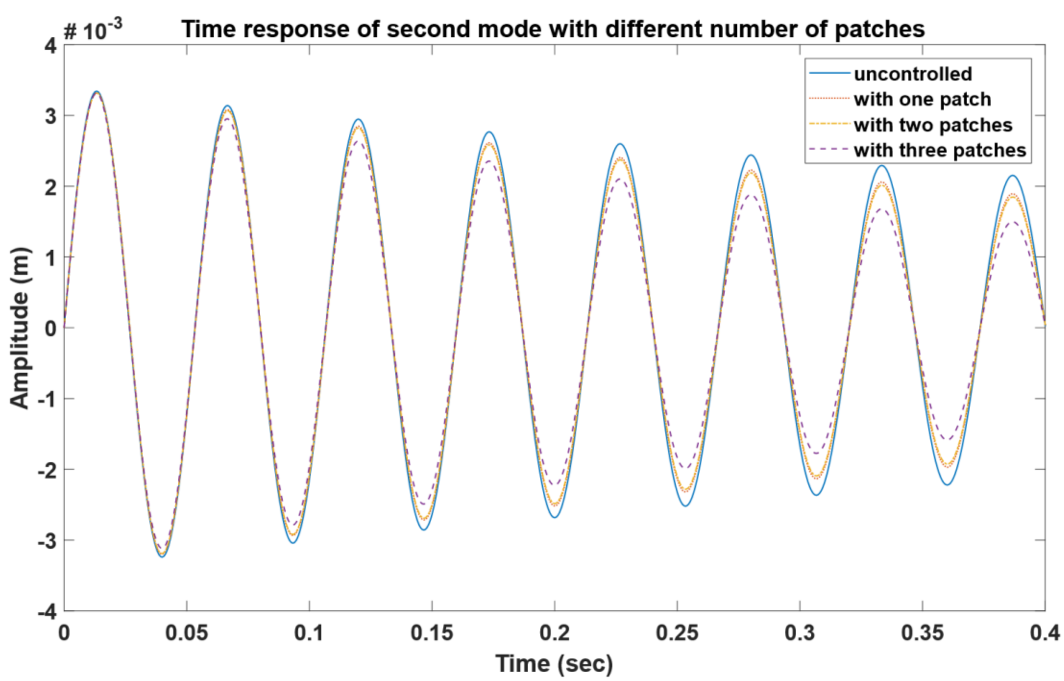

Figure 4. Time response of second mode

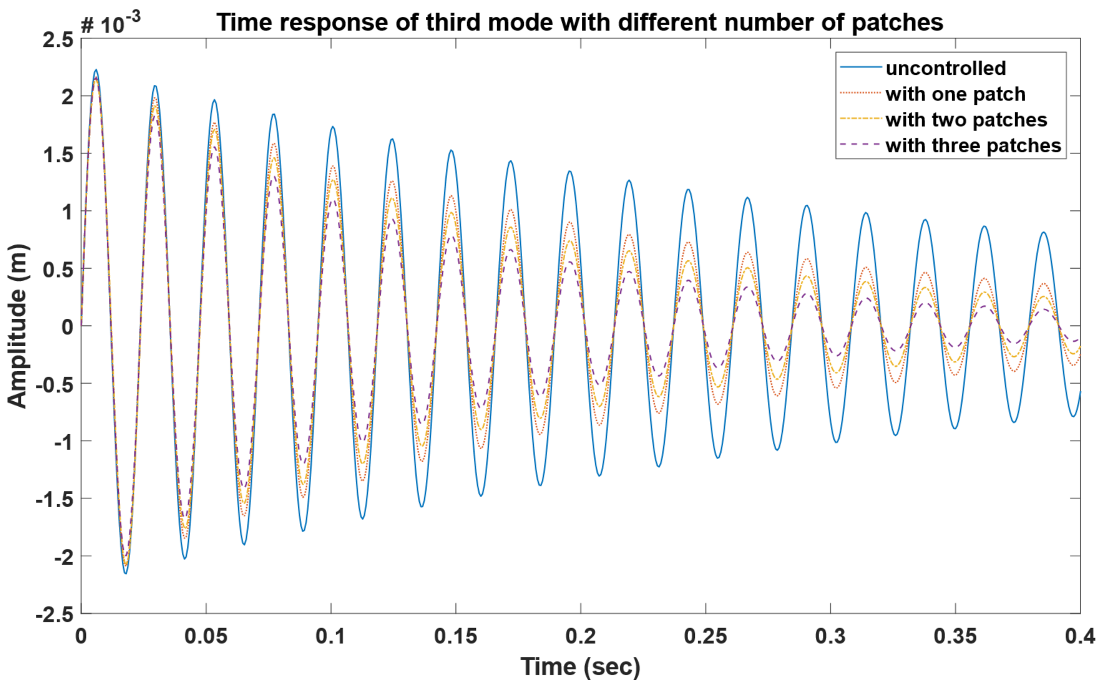

Figure 5. Time response of third mode

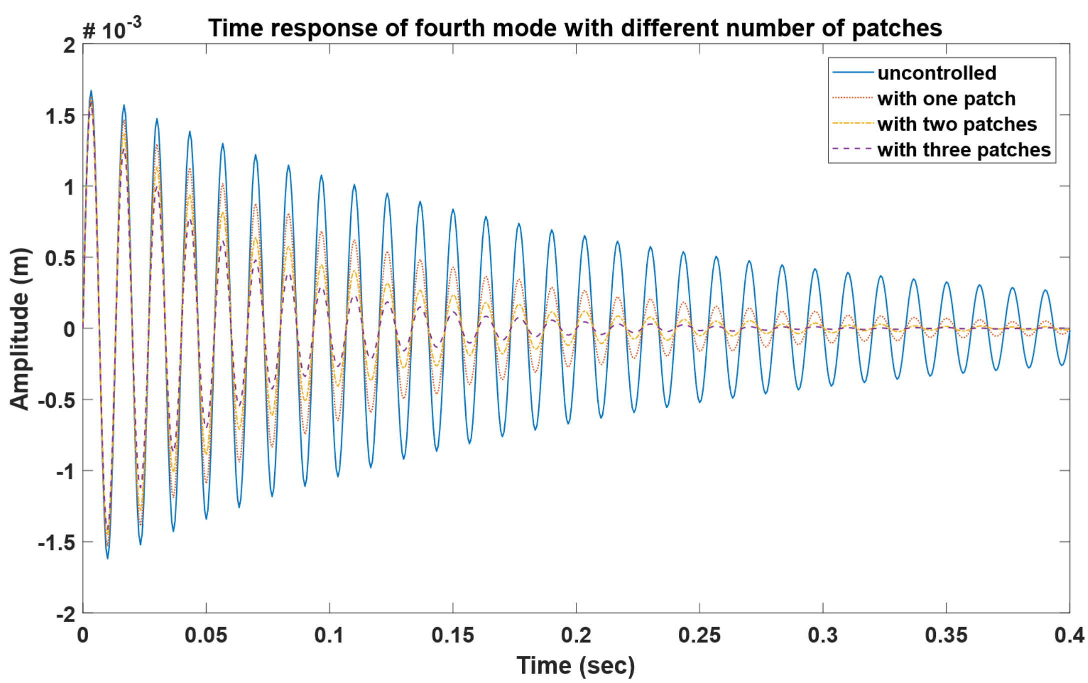

Figure 6. Time response of fourth mode

The peak amplitudes of first four vibration modes with and without control using up to three sensor/actuator pairs are shown in Table 4. As it can be observed, the peak amplitudes reduce with increasing number of patches for modes 1 to 3. This is not true for mode 4 wherein the peak amplitude increases if the number of patch pairs is more than one.

Table 4. Peak amplitudes (m) after 1 sec

Number of patch pairs, m	**Mode 1**	**Mode 2**	**Mode 3**	**Mode 4**
0	0.0049	0.0010	1.5922e-04	1.4991e-05
1	0.0048	0.00072	2.0041e-05	7.6554e-07
2	0.0047	0.00067	8.5234e-06	9.2139e-07
3	0.0046	0.00039	2.0594e-06	9.7338e-07

5 CONCLUSIONS

- Increasing number of piezoelectric patches results in increased vibration suppression for modes 1, 2 & 3. However, for mode 4 amplitudes increase if the number of patch pairs is more than one.

- The maximum reduction in modal amplitude with three patch pairs for mode 1 is only -6.12% whereas it is - 61% for mode 2, -98.7 % for mode 3 and -93.5% for mode 4.

- Depending upon the degree of amplitude reduction required for modes of interest, a decision can be made regarding performance improvement versus cost.

6 REFERENCES

[1] Gupta, Vivek, Manu Sharma, and Nagesh Thakur. "Optimization Criteria for Optimal Placement of Piezoelectric Sensors and Actuators on a Smart Structure: A Technical Review." Journal of Intelligent Material Systems and Structures 21.12 (2010): 1227-243.

[2] Crawley, Edward F., and Javier De Luis. "Use of piezoelectric actuators as elements of intelligent structures." AIAA journal 25.10 (1987): 1373-1385.

[3] Ning, Hao Hua. "Optimal Number and Placements of Piezoelectric Patch Actuators in Structural Active Vibration Control." Engineering Computations 21.6 (2004): 651-65.

[4] Li, Q.s., D.k. Liu, J. Tang, N. Zhang, and C.m. Tam. "Combinatorial Optimal Design of Number and Positions of Actuators in Actively Controlled Structures Using Genetic Algorithms." Journal of Sound and Vibration 270.4-5 (2004): 611-24.

[5] Yan, Y. J., and L. H. Yam. "Optimal Design of Number and Locations of Actuators in Active Vibration Control of a Space Truss." Smart Materials and Structures 11.4 (2002): 496-503.

[6] Tzou, H. S. Distributed Sensing and Control of Continua. Dordrecht: Kluwer Academic, 1993. Print.

[7] Kumar, K. Ramesh, and S. Narayanan. "Active Vibration Control of Beams with Optimal Placement of Piezoelectric Sensor/actuator Pairs." Smart Materials and Structures 17.5 (2008): 055008.

[8] Yang, Yaowen, Zhanli Jin, and Chee Kiong Soh. "Integrated Optimal Design of Vibration Control System for Smart Beams Using Genetic Algorithms." Journal of Sound and Vibration 282.3-5 (2005): 1293-307.

[9] A.C. Lee, S.T. Chen, Collocated sensor/actuator positioning and feedback design in the control of flexible structure system, Journal of Vibration and Acoustics 116 (1994) 146–154.

[10] "Documentation." Genetic Algorithm - MATLAB & Simulink. The MathWorks, Inc., 30 Apr. 2017. <https://www.mathworks.com/help/gads/genetic-algorithm.html>.

[11] Goldberg, David Edward. Genetic Algorithms in Search, Optimization, and Machine Learning. Boston: Addison-Wesley, 2012. Print.

APPENDICES

APPENDIX A – MATLAB CODES

```
% MAE 538 Design of Smart Material Systems - Course Project
% Active vibration control of a beam using smart materials
% Vinod Kumar Singla 4/22/2017
clear all;clc;close all;
% %% Optimal placement for one pair/two patches
% lb = zeros(1,2); % lower bounds on individual design variables
% ub = 0.5.*ones(1,2); % upper bounds on individual design variables
% opts = gaoptimset('PlotFcn',{@gaplotbestf,@gaplotstopping},'Generations',200,'TolFun',1e-
6,'TolCon',1e-6);
% fitnessfcn = @objF1;
% nvars = 2; Lp = 0.1; % length of a piezopatch (100mm) = 1/5th beam length
% nonlcon = [];
% Aeq = [-1,1];
% beq = Lp;
% A = [1 -1];
% b = [0];
% [x,fval,exitflag,output] = ga(fitnessfcn,nvars,A,b,Aeq,beq,lb,ub,nonlcon,opts)
% [x,fval]'

% %% Optimal placement for two pairs/four patches
% lb = zeros(1,4); % lower bounds on individual design variables
% ub = 0.5.*ones(1,4); % upper bounds on individual design variables
% opts = gaoptimset('PlotFcn',{@gaplotbestf,@gaplotstopping},'Generations',200,'TolFun',1e-
6,'TolCon',1e-6);
% fitnessfcn = @objF2;
% nvars = 4; Lp = 0.1; % length of a piezopatch (50mm) = 1/10th beam length
% nonlcon = [];
% Aeq = [-1,1,0,0;0,0,-1,1];
% beq = [Lp;Lp];
% A = [1 -1 0 0;0 0 1 -1;0 1 -1 0];
% b = [0;0;0];
% [x,fval,exitflag,output] = ga(fitnessfcn,nvars,A,b,Aeq,beq,lb,ub,nonlcon,opts)
% [x,fval]'

% Optimal placement for three pairs/six patches
% lb = zeros(1,6); % lower bounds on individual design variables
% ub = 0.5.*ones(1,6); % upper bounds on individual design variables
% opts = gaoptimset('PlotFcn',{@gaplotbestf,@gaplotstopping},'Generations',200,'TolFun',1e-
6,'TolCon',1e-6);
% fitnessfcn = @objF3;
% nvars = 6; Lp = 0.1; % length of a piezopatch (50mm) = 1/10th beam length
% nonlcon = [];
% Aeq = [-1,1,0,0,0,0;0,0,-1,1,0,0;0,0,0,0,-1,1];
% beq = [Lp;Lp;Lp];
% A = [1 -1 0 0 0 0;0 0 1 -1 0 0;0 0 0 0 1 -1;...
%     0 1 -1 0 0 0;0 0 0 1 -1 0];
% b = [0;0;0;0;0];
% [x,fval,exitflag,output] = ga(fitnessfcn,nvars,A,b,Aeq,beq,lb,ub,nonlcon,opts)
% [x,fval]'
```

```
% MAE 538 Design of Smart Material Systems - Course Project
% Active vibration control of a beam using smart materials
% Vinod Kumar Singla 4/22/2017
% Note: X = [x11 x12 x21 x22 x31 x32 . . . xm1 xm2]
% # of Piezoelectric patches = m, # of modes considered = 4

function f = objF1(X)
%% Beam properties
rho_b = 1190; % density, kg/^3
E_b = 3.1028e9; % young's modulus, Pa
v_b = 0.3; % poisson's ratio, dimensionless
t_b = 1.6e-3; % thickness, m
L_b = 0.5; % length, m
b = 0.01; % width, m
J_b = b*t_b^3/12; % Area Moment of Inertia
A_b = b*t_b; % cross sectional area of the beam
zeta = diag([0.01,0.01,0.01,0.01]); % damping ratio, dimensionless

%% Piezoelectric patch properties
rho = 1800; % density, kg/^3
E = 2e9; % young's modulus, Pa
d31 = 2.3e-11; %piezoelectric constant, m/V
h31 = 4.32e8; %piezoelectric constant, V/m
v = 0.3; % poisson's ratio, dimensionless
t = 4e-5; % thickness, m

%% Derived constants
Ka = b*((t_b+t)/2)*d31*E;
Ks1 = - t*h31*((t_b+t)/2)/(X(2)-X(1));

%% Natural frequencies for first 4 modes
wj = (pi/L_b)^2*sqrt(E_b*J_b/(rho_b*A_b));
W = wj.*(diag([1,2^2,3^2,4^2]));

%% Mode shape derivative differences for all elements
% Element 1
U1diff21 = (sqrt(2/(rho_b*L_b*A_b)))*(1*pi/L_b)*(cos((1*pi*X(2))/L_b)-cos((1*pi*X(1))/L_b));
U2diff21 = (sqrt(2/(rho_b*L_b*A_b)))*(2*pi/L_b)*(cos((2*pi*X(2))/L_b)-cos((2*pi*X(1))/L_b));
U3diff21 = (sqrt(2/(rho_b*L_b*A_b)))*(3*pi/L_b)*(cos((3*pi*X(2))/L_b)-cos((3*pi*X(1))/L_b));
U4diff21 = (sqrt(2/(rho_b*L_b*A_b)))*(4*pi/L_b)*(cos((4*pi*X(2))/L_b)-cos((4*pi*X(1))/L_b));

%% Open loop matrices
B_ = Ka.*[U1diff21;U2diff21;U3diff21;U4diff21];

C_ = Ks1.*[U1diff21,U2diff21,U3diff21,U4diff21];

A = vertcat([zeros(4),eye(4)],[-W*W,-2*zeta*W]);
B = [zeros(4,1);B_];
C = [C_,zeros(1,4)];
Q = vertcat([W*W,zeros(4)],[zeros(4),eye(4)]);

%% Close loop matrices
G = .4;
Ac = double(vertcat([zeros(4),eye(4)],[-W*W,B_*G*C_-2.*zeta*W]));

%% Initial conditions
n0 = [0,0,0,0]; n0_d = [0.2,0.4,0.6,0.8];n = [n0,n0_d];
P = lyap(double(Ac)',-double(Q)); % The inbuilt function is used to boost speed
f = max(-double(n*P*n'),0);
end
```

```
% MAE 538 Design of Smart Material Systems - Course Project
% Active vibration control of a beam using smart materials
% Vinod Kumar Singla 4/22/2017
% Note: X = [x11 x12 x21 x22 x31 x32 . . . xm1 xm2]
% # of Piezoelectric patches = m, # of modes considered = 4

function f = objF2(X)
%% Beam properties
rho_b = 1190; % density, kg/^3
E_b = 3.1028e9; % young's modulus, Pa
v_b = 0.3; % poisson's ratio, dimensionless
t_b = 1.6e-3; % thickness, m
L_b = 0.5; % length, m
b = 0.01; % width, m
J_b = b*t_b^3/12; % Area Moment of Inertia
A_b = b*t_b; % cross sectional area of the beam
zeta = diag([0.01,0.01,0.01,0.01]); % damping ratio, dimensionless

%% Piezoelectric patch properties
rho = 1800; % density, kg/^3
E = 2e9; % young's modulus, Pa
d31 = 2.3e-11; %piezoelectric constant, m/V
h31 = 4.32e8; %piezoelectric constant, V/m
v = 0.3; % poisson's ratio, dimensionless
t = 4e-5; % thickness, m

%% Derived constants
Ka = b*((t_b+t)/2)*d31*E;
Ks1 = - t*h31*((t_b+t)/2)/(X(2)-X(1));
Ks2 = - t*h31*((t_b+t)/2)/(X(4)-X(3));

%% Natural frequencies for first 4 modes
wj = (pi/L_b)^2*sqrt(E_b*J_b/(rho_b*A_b));
W = wj.*(diag([1,2^2,3^2,4^2]));

%% Mode shape derivative differences for all elements
% Element 1
U1diff21 = (sqrt(2/(rho_b*L_b*A_b)))*(1*pi/L_b)*(cos((1*pi*X(2))/L_b)-cos((1*pi*X(1))/L_b));
U2diff21 = (sqrt(2/(rho_b*L_b*A_b)))*(2*pi/L_b)*(cos((2*pi*X(2))/L_b)-cos((2*pi*X(1))/L_b));
U3diff21 = (sqrt(2/(rho_b*L_b*A_b)))*(3*pi/L_b)*(cos((3*pi*X(2))/L_b)-cos((3*pi*X(1))/L_b));
U4diff21 = (sqrt(2/(rho_b*L_b*A_b)))*(4*pi/L_b)*(cos((4*pi*X(2))/L_b)-cos((4*pi*X(1))/L_b));

% Element 2
U1diff43 = (sqrt(2/(rho_b*L_b*A_b)))*(1*pi/L_b)*(cos((1*pi*X(4))/L_b)-cos((1*pi*X(3))/L_b));
U2diff43 = (sqrt(2/(rho_b*L_b*A_b)))*(2*pi/L_b)*(cos((2*pi*X(4))/L_b)-cos((2*pi*X(3))/L_b));
U3diff43 = (sqrt(2/(rho_b*L_b*A_b)))*(3*pi/L_b)*(cos((3*pi*X(4))/L_b)-cos((3*pi*X(3))/L_b));
U4diff43 = (sqrt(2/(rho_b*L_b*A_b)))*(4*pi/L_b)*(cos((4*pi*X(4))/L_b)-cos((4*pi*X(3))/L_b));

%% Open loop matrices
B_ = Ka.*[U1diff21,U1diff43;...
    U2diff21,U2diff43;...
    U3diff21,U3diff43;...
    U4diff21,U4diff43];

C_ = [Ks1.*[U1diff21,U2diff21,U3diff21,U4diff21];...
    Ks2.*[U1diff43,U2diff43,U3diff43,U4diff43]];

A = vertcat([zeros(4),eye(4)],[-W*W,-2*zeta*W]);
B = [zeros(4,2);B_];
C = [C_,zeros(2,4)];
Q = vertcat([W*W,zeros(4)],[zeros(4),eye(4)]);

%% Close loop matrices
G = [.4,0.4;0,0.4];
Ac = double(vertcat([zeros(4),eye(4)],[-W*W,B_*G*C_-2.*zeta*W]));

%% Initial conditions
n0 = [0,0,0,0]; n0_d = [0.2,0.4,0.6,0.8];n = [n0,n0_d];
P = lyap(double(Ac)',-double(Q)); % The inbuilt function is used to boost speed
f = max(-double(n*P*n'),0);
end
```

```
% MAE 538 Design of Smart Material Systems - Course Project
% Active vibration control of a beam using smart materials
% Vinod Kumar Singla 4/22/2017
% Note: X = [x11 x12 x21 x22 x31 x32 . . . xm1 xm2]
% # of Piezoelectric patches = m, # of modes considered = 4

function f = objF3(X)
%% Beam properties
rho_b = 1190; % density, kg/^3
E_b = 3.1028e9; % young's modulus, Pa
v_b = 0.3; % poisson's ratio, dimensionless
t_b = 1.6e-3; % thickness, m
L_b = 0.5; % length, m
b = 0.01; % width, m
J_b = b*t_b^3/12; % Area Moment of Inertia
A_b = b*t_b; % cross sectional area of the beam
zeta = diag([0.01,0.01,0.01,0.01]); % damping ratio, dimensionless

%% Piezoelectric patch properties
rho = 1800; % density, kg/^3
E = 2e9; % young's modulus, Pa
d31 = 2.3e-11; %piezoelectric constant, m/V
h31 = 4.32e8; %piezoelectric constant, V/m
v = 0.3; % poisson's ratio, dimensionless
t = 4e-5; % thickness, m

%% Derived constants
Ka = b*((t_b+t)/2)*d31*E; Ks1 = - t*h31*((t_b+t)/2)/(X(2)-X(1));
Ks2 = - t*h31*((t_b+t)/2)/(X(4)-X(3)); Ks3 = - t*h31*((t_b+t)/2)/(X(6)-X(5));

%% Natural frequencies for first 4 modes
wj = (pi/L_b)^2*sqrt(E_b*J_b/(rho_b*A_b)); W = wj.*(diag([1,2^2,3^2,4^2]));

%% Mode shape derivative differences for all elements
% Element 1
U1diff21 = (sqrt(2/(rho_b*L_b*A_b)))*(1*pi/L_b)*(cos((1*pi*X(2))/L_b)-cos((1*pi*X(1))/L_b));
U2diff21 = (sqrt(2/(rho_b*L_b*A_b)))*(2*pi/L_b)*(cos((2*pi*X(2))/L_b)-cos((2*pi*X(1))/L_b));
U3diff21 = (sqrt(2/(rho_b*L_b*A_b)))*(3*pi/L_b)*(cos((3*pi*X(2))/L_b)-cos((3*pi*X(1))/L_b));
U4diff21 = (sqrt(2/(rho_b*L_b*A_b)))*(4*pi/L_b)*(cos((4*pi*X(2))/L_b)-cos((4*pi*X(1))/L_b));

% Element 2
U1diff43 = (sqrt(2/(rho_b*L_b*A_b)))*(1*pi/L_b)*(cos((1*pi*X(4))/L_b)-cos((1*pi*X(3))/L_b));
U2diff43 = (sqrt(2/(rho_b*L_b*A_b)))*(2*pi/L_b)*(cos((2*pi*X(4))/L_b)-cos((2*pi*X(3))/L_b));
U3diff43 = (sqrt(2/(rho_b*L_b*A_b)))*(3*pi/L_b)*(cos((3*pi*X(4))/L_b)-cos((3*pi*X(3))/L_b));
U4diff43 = (sqrt(2/(rho_b*L_b*A_b)))*(4*pi/L_b)*(cos((4*pi*X(4))/L_b)-cos((4*pi*X(3))/L_b));

% Element 3
U1diff65 = (sqrt(2/(rho_b*L_b*A_b)))*(1*pi/L_b)*(cos((1*pi*X(6))/L_b)-cos((1*pi*X(5))/L_b));
U2diff65 = (sqrt(2/(rho_b*L_b*A_b)))*(2*pi/L_b)*(cos((2*pi*X(6))/L_b)-cos((2*pi*X(5))/L_b));
U3diff65 = (sqrt(2/(rho_b*L_b*A_b)))*(3*pi/L_b)*(cos((3*pi*X(6))/L_b)-cos((3*pi*X(5))/L_b));
U4diff65 = (sqrt(2/(rho_b*L_b*A_b)))*(4*pi/L_b)*(cos((4*pi*X(6))/L_b)-cos((4*pi*X(5))/L_b));

%% Open loop matrices
B_ = Ka.*[U1diff21,U1diff43,U1diff65;...
    U2diff21,U2diff43,U2diff65;...
    U3diff21,U3diff43,U3diff65;...
    U4diff21,U4diff43,U4diff65];

C_ = [Ks1.*[U1diff21,U2diff21,U3diff21,U4diff21];...
    Ks2.*[U1diff43,U2diff43,U3diff43,U4diff43];...
    Ks3.*[U1diff65,U2diff65,U3diff65,U4diff65]];

A = vertcat([zeros(4),eye(4)],[-W*W,-2*zeta*W]);     B = [zeros(4,3);B_];
C = [C_,zeros(3,4)]; Q = vertcat([W*W,zeros(4)],[zeros(4),eye(4)]);

%% Close loop matrices
G = [.4,0,0;0,0.4,0.0342;0,0,0.4];
Ac = double(vertcat([zeros(4),eye(4)],[-W*W,B_*G*C_-2.*zeta*W]));

%% Initial conditions
n0 = [0,0,0,0]; n0_d = [0.2,0.4,0.6,0.8];n = [n0,n0_d];
P = lyap(double(Ac)',-double(Q)); % The inbuilt function is used to boost speed
f = max(-double(n*P*n'),0);
end
```

APPENDIX B – OPTIMAL DESIGN CANDIDATES

Table 5. Optimal design candidates for one pair of sensor/actuator

Design	x0	x1	x2	x3
x11 (m)	**0.027**	0.027	0.027	0.027
x12 (m)	**0.127**	0.127	0.127	0.127
E	**0.192**	0.192	0.192	0.192

Table 6. Optimal design candidates for two pairs of sensors/actuators

Design	x0	x1	x2	x3	x4	x5	x6	x7	x8	x9
x11 (m)	0.029	**0.026**	0.029	0.034	0.027	0.100	0.031	0.101	0.104	0.027
x12 (m)	0.129	**0.126**	0.129	0.134	0.127	0.200	0.131	0.201	0.204	0.127
x21 (m)	0.299	**0.302**	0.300	0.293	0.300	0.373	0.298	0.370	0.370	0.300
x22 (m)	0.399	**0.402**	0.400	0.393	0.400	0.473	0.398	0.470	0.470	0.400
E	0.166	**0.166**	0.166	0.167	0.166	0.166	0.166	0.166	0.167	0.166

Table 7. Optimal design candidates for three pairs of sensors/actuators

Design	x0	x1	x2	x3	x4	x5	x6	x7	x8	x9
x11 (m)	0.033	**0.033**	0.036	0.034	0.034	0.039	0.034	0.034	0.035	0.033
x12 (m)	0.133	**0.133**	0.136	0.134	0.134	0.139	0.134	0.134	0.135	0.133
x21 (m)	0.254	**0.141**	0.143	0.142	0.146	0.144	0.144	0.261	0.141	0.258
x22 (m)	0.354	**0.241**	0.243	0.242	0.246	0.244	0.244	0.361	0.241	0.358
x31 (m)	0.364	**0.366**	0.367	0.366	0.369	0.354	0.355	0.366	0.363	0.367
x32 (m)	0.464	**0.466**	0.467	0.466	0.469	0.454	0.455	0.466	0.463	0.467
E	0.140	**0.139**	0.139	0.139	0.139	0.140	0.140	0.139	0.139	0.139

***